Emerging Active Regions Observed by SDO/HMI for Helioseismology

H. Schunker[1] & D.C. Braun[2] & A.C. Birch[1]

1. Max Planck Institute for Solar System Research, Göttingen, Germany
2. North West Research Associates, Boulder, U.S.A

schunker@mps.mpg.de

Abstract

The dynamics of the formation, evolution and decay of active regions on the Sun remains unknown. Two main theories of active region formation exist: the emergence of a buoyant flux tube from the base of the convection zone which pierces the surface, forming bi-polar active regions; and the passive conglomeration of flux by the surface convection to form active regions. Detecting and understanding subsurface changes due to active regions would help to constrain the theories. Helioseismology is the use of acoustic waves to probe the subsurface structure and is the only tool available to 'see' the interior of the Sun. Statistical studies of emerging active regions using helioseismology can help to isolate the common features of often complex individual emergences, in an effort to constrain the emergence process. Motivated by the previous statistical analysis of [1], [2] and [3] using MDI magnetograms and ground-based GONG Doppler velocity observations, in this poster we describe our catalogue of emerging active regions observed by SDO/HMI for use in helioseismology. In this dataset, the emerging active regions have been tracked further back in time before the emergence, allowing us to probe deeper below the surface using helioseismology.

1. Selection criteria for Emerging Active Regions (EARs)

We first identified Emerging Active Regions (EARs) from NOAA sunspot observation records from April 2010 to November 2012 that needed to satisfy some conditions:

- the first instance of a record for an active region must occur within $58°$ longitudinal distance from the central meridian (allowing for observations at least one day either side) before reaching $65°$ longitudinal distance from central meridian, beyond which centre-to-limb effects become significant;
- the active region must reach a size of at least 10 micro hemispheres;
- lastly, to ensure that the emergence did not occur within, or too close to, an existing active region we required that MTOT_c must rise sharply to some maximum value within 36 hours of the time of the first NOAA record of the region. To do this, we retrieved the flux as a function of time as given by MTOT keyword for the active region in the hmi.mharp_720s series stored in the Data Record Management System (DRMS) produced by the HMI team [4], and then normalised the flux so that $\mathrm{MTOT}_c = \mathrm{MTOT}/\cos\theta$, where θ is the angular distance to disk centre.

This resulted in a final list of 105 emerging active regions in the catalogue. See the print outs attached to this poster for the complete list of EARs and CRs.

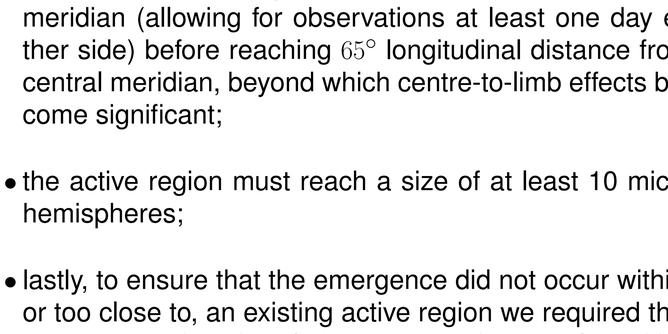

Figure 1: *The average magnetic field for the final 105 EARs in the catalogue 16 hours before emergence (left), at the emergence time (middle) and 16 hours after emergence (right). The EARs in the southern hemisphere have had their polarity reversed and the maps reversed in the latitudinal direction, showing the average tilt angle towards the equator in time. The magnetic field is limited to the range ± 100 G.*

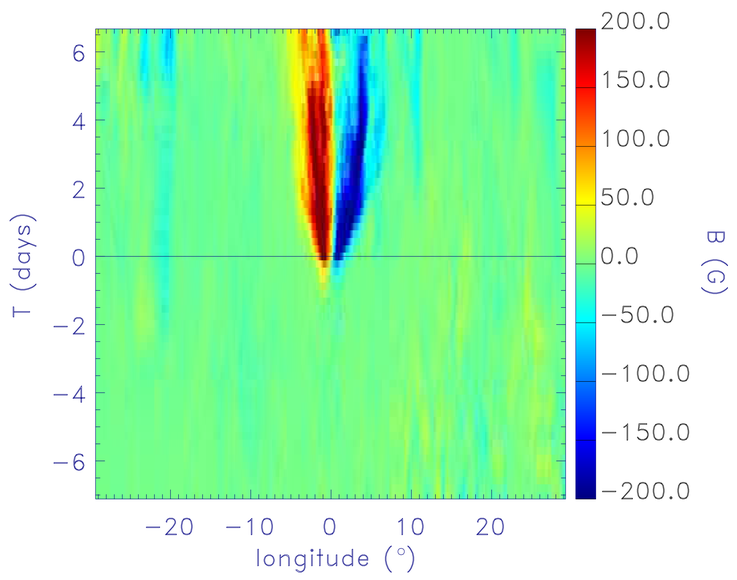

Figure 2: *A cut at zero degrees latitude through the average magnetic field maps, some of which are shown in Fig. 1, as a function of time relative to the emergence.*

The time of emergence, T0, was defined as when the MTOT_c reaches 10% of the maximum value within 36 hours of T0. The emergence time and location was defined based on the hmi.mharp_720s series which has a cadence of 720 seconds.

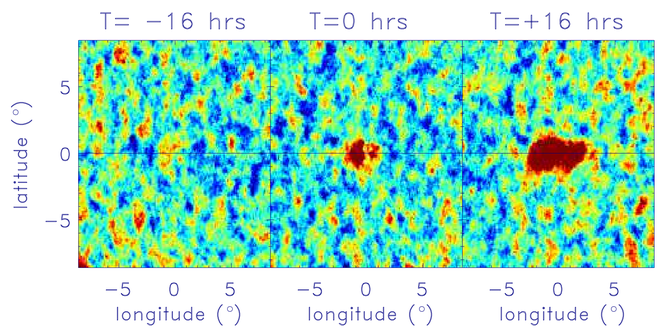

Figure 3: *The average Doppler velocity for the final EARs 16 hours before emergence, at the emergence time and 16 hours after emergence. The Doppler velocity is limited to the range ± 50 m/s, where red is red-shift and blue is blue-shift.*

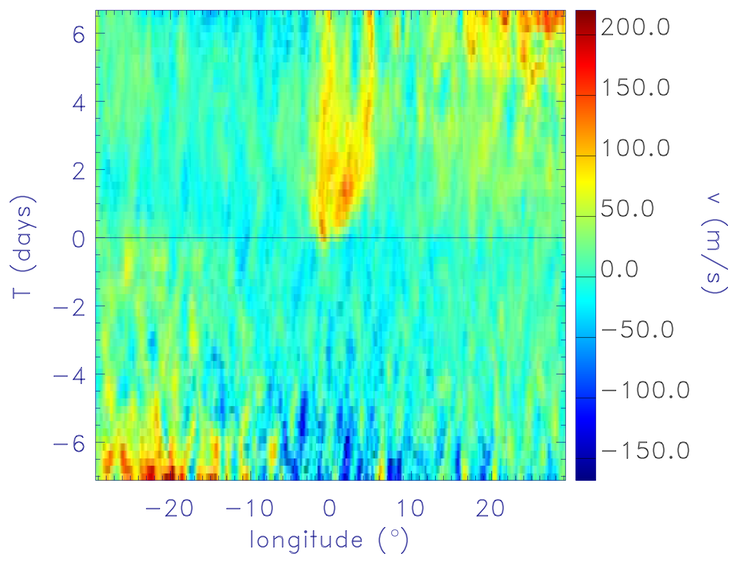

Figure 4: *A cut at zero degrees latitude through the average Doppler velocity maps, some of which are shown in Fig. 3, as a function of time relative to the emergence.*

2. Selection criteria for Control Regions (CRs)

For each EAR we then selected a corresponding control region (CR) with exactly the same latitude and longitudinal distance from central meridian at it's 'emergence time'. The requirements for the control region are,

1. that the CR did not lead to an emerging active region;
2. the artificial 'emergence time' must occur at least 2 days before or after the emergence time of the EAR. The standard deviation of the time separating the two regions is 8 days;
3. must not have any numbered HARP (Helioseismic Active Region Patch) region within $30°$ at the emergence time or six days before;
4. ideally the pre-emergence magnetic flux within a $10°$ radius should not be much stronger than the EAR, although this is not always the case.

The selection of control regions was done automatically, however it was difficult to find satisfactory CRs for some EARs, and so some were handpicked.

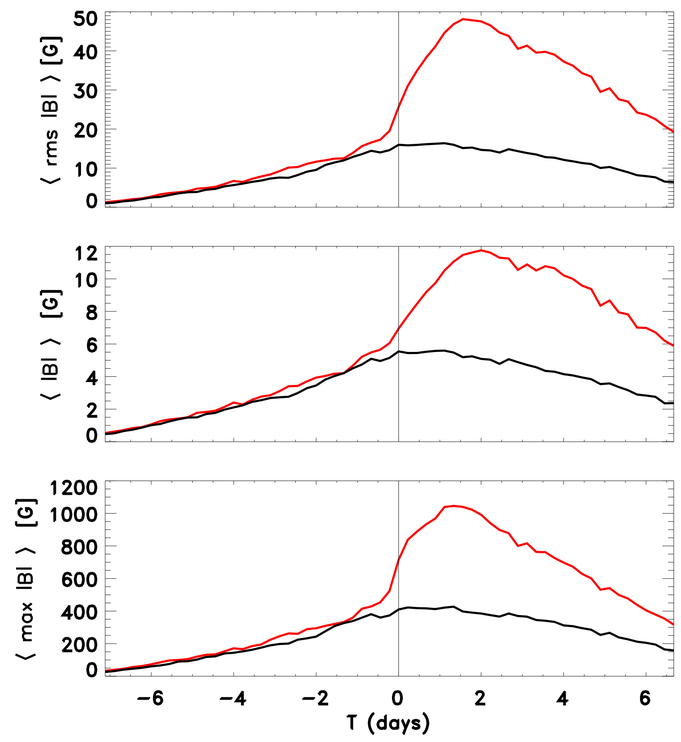

Figure 5: *Properties of the absolute value of the magnetic field within the central $10°$ of the average of the emerging active regions (red curve) and the average of the control regions (black curve) as a function of time relative to the emergence, indicated by the vertical line.*

3. Data reduction

We tracked the latitudes and longitudes of the selected EARs and CRs at the Carrington rotation rate over intervals of 6.825 hours (547 frames with a cadence of 45 seconds), spaced 5.3375 hours apart (427 frames). Thus, there is a 1.5 hour (120 frame) overlap between datacubes. Each map in the datacube has been Postel projected from full-disk observations onto $60°\times60°$ maps (512×512 pixels where the pixel size is 0.002 solar radians) centred at the specified longitude and latitude for each EAR and CR.

We mapped full-disk SDO/HMI magnetogram, Dopplergram and intensity observations onto a Postel projection centred at the longitude and latitude of the EAR (or the CR) with a 45 second cadence. The emergence time occurs 28.5 minutes (39 frames) before the end of the datacube labeled with time interval TI=−01 and 1 hour and 45 seconds (81 frames) after the beginning of the datacube labelled TI=+00. The average magnetic field as a function of time is shown in Fig. 5.

4. Summary

This catalogue of emerging active regions including mapped and tracked datacubes of Doppler velocity, line-of-sight magnetic field and intensity observations from SDO/HMI are available as DRMS data series'. This study follows on from the previous statistical study of [1], [2] and [3]. The data series is designed for statistical helioseismic studies, but is also useful for other studies for example, of the magnetic field during emergence, as well as individual case studies or sub-classifications of emerging active regions, supergranules and small plage regions.

References

[1] K.D. Leka et al. Helioseismology of Pre-emerging Active Regions. I. Overview, Data, and Target Selection Criteria *Astrophys. J.*, 762, 2013.

[2] A.C. Birch et al. Helioseismology of Pre-emerging Active Regions. II. Average Emergence Properties *Astrophys. J.*, 762, 2013.

[3] G. Barnes et al. Helioseismology of Pre-emerging Active Regions. III. Statistical Analysis *Astrophys. J.*, 786, 2014.

[4] M.G. Bobra et al. The Helioseismic and Magnetic Imager (HMI) Vector Magnetic Field Pipeline: SHARPs - Space-Weather HMI Active Region Patches *Sol. Phys.*,289, 2014.